Geophysical Research Letters

RESEARCH LETTER
10.1029/2025GL115394

Does Foreshock Identification Depend on Seismic Monitoring Capability?

Xin Cui[1,2], Zefeng Li[1,3], Jean-Paul Ampuero[2], and Louis De Barros[2]

[1]School of Earth and Space Sciences, University of Science and Technology of China, Hefei, China, [2]Université Côte d'Azur, Observatoire de la Côte d'Azur, IRD, CNRS, Géoazur, France, [3]Mengcheng National Geophysical Observatory, University of Science and Technology of China, Mengcheng, China

Abstract Foreshocks, though well-documented phenomena preceding many large earthquakes, have limited forecasting utility due to their non-pervasive occurrence and non-distinctive characteristics. Using California as an example, we investigate how seismic monitoring capability, particularly the completeness magnitude (M_c), influences the inferred proportion of mainshocks with foreshocks (P_f). We test four foreshock identification methods, namely the fixed-window, nearest neighbor clustering, empirical statistical (ES) methods and the epidemic-type aftershock sequence (ETAS) model. The fixed-window method shows P_f decreasing with higher M_c due to the misclassification of background events as foreshocks. In contrast, clustering and ES methods yield relatively stable P_f across different M_c values. The ETAS model suggests that many foreshocks in California are associated with aseismic driving processes, but the identification of the processes diminishes at high M_c. These results show that improved seismic monitoring capability does not significantly increase P_f but is crucial for distinguishing processes driving foreshocks.

Plain Language Summary Foreshocks are seismic events that sometimes occur before large earthquakes. However, they are not always present and do not have clear distinguishing features, limiting their usefulness for earthquake forecasting. We examine how the earthquake monitoring capability affects the observed proportion of large earthquakes that have foreshocks. Using seismic data from California, we apply four foreshock identification methods: the fixed-window method, nearest neighbor clustering, empirical statistical (ES) methods, and the epidemic-type aftershock sequence (ETAS) model. Our results show that the fixed-window method leads to less observations of large earthquakes with foreshocks when the monitoring capability is worse. In contrast, clustering and ES methods provide more stable proportions of large earthquakes with foreshocks even when the monitoring capability varies. And the ETAS model suggests that many foreshocks in Califorina are associated with aseismic processes. However, poor monitoring capability limits the ability to distinguish between foreshocks driven by aseismic processes and those triggered by cascading seismic failure through stress transfer. These findings indicate that while enhanced seismic monitoring does not necessarily lead to a higher proportion of identified foreshocks, it is essential for understanding the underlying physical mechanisms driving foreshock activity.

Key Points:

- We assess the impact of magnitude of completeness (M_c) on multiple foreshock identification methods in California
- Foreshock dependence on M_c is weak in some methods because the magnitude difference between mainshock and largest foreshock is small
- Foreshocks driven by aseismic processes are numerous in California, but their detectability diminishes at high M_c

Supporting Information:

Supporting Information may be found in the online version of this article.

Correspondence to:

Z. Li,
zefengli@ustc.edu.cn

Citation:

Cui, X., Li, Z., Ampuero, J.-P., & De Barros, L. (2025). Does foreshock identification depend on seismic monitoring capability? *Geophysical Research Letters*, *52*, e2025GL115394. https://doi.org/10.1029/2025GL115394

Received 13 FEB 2025
Accepted 26 MAY 2025

Author Contributions:

Conceptualization: Xin Cui, Zefeng Li, Jean-Paul Ampuero, Louis De Barros
Data curation: Xin Cui
Formal analysis: Louis De Barros
Funding acquisition: Zefeng Li
Investigation: Xin Cui, Jean-Paul Ampuero
Methodology: Xin Cui, Jean-Paul Ampuero
Project administration: Zefeng Li
Software: Xin Cui
Supervision: Zefeng Li, Jean-Paul Ampuero
Validation: Xin Cui, Jean-Paul Ampuero, Louis De Barros

1. Introduction

Foreshocks are small to moderate earthquakes that occur shortly before a mainshock (Mogi, 1963) and are considered promising for short-term earthquake forecasting (Dodge et al., 1995; Kato et al., 2012; Ruiz et al., 2014; Wang et al., 2006). Laboratory experiments commonly observe precursory slip events resembling foreshocks, interpreted as nucleation processes preceding ultimate rupture (Bolton et al., 2019; Goebel et al., 2024; Marty et al., 2023). Similarly, theoretical fault friction models, such as the rate-and-state framework, predict an aseismic nucleation phase before dynamic rupture (Ampuero & Rubin, 2008; Dieterich, 1994; He et al., 2023; Rubin & Ampuero, 2005). However, the question of how pervasive are foreshocks remains debated: estimates from past studies range from 10% to 70% (Abercrombie & Mori, 1996; Chen & Shearer, 2016; Reasenberg, 1999; Trugman & Ross, 2019; Wetzler, Lay, et al., 2023).

Foreshock detection is affected by seismic monitoring capability (Mignan, 2014; Trugman & Ross, 2019). However, seismic monitoring capability affects the detection of both foreshock and background events, raising the critical question of whether increasing monitoring capability leads to more mainshocks being identified as having foreshocks. A meta-analysis of 37 studies by Mignan (2014) found that lower magnitude thresholds

Visualization: Xin Cui, Zefeng Li
Writing – original draft: Xin Cui, Zefeng Li
Writing – review & editing: Zefeng Li, Jean-Paul Ampuero, Louis De Barros

correlate with a higher proportion of mainshocks identified as having foreshocks (P_f), suggesting many foreshocks remain undetected due to limited monitoring capability. Using a template-matching enhanced catalog (QTM; Ross et al., 2019), Trugman and Ross (2019) reported that P_f is 72% in Southern California, much higher than the 53% reported by Chen and Shearer (2016). However, reanalyzes of the same QTM catalog with methods accounting for background seismicity fluctuations found lower foreshock proportions, ranging from 20% to 40% (van den Ende & Ampuero, 2020).

Moreover, foreshock mechanisms are still a matter of research (Bouchon et al., 2011; Ellsworth & Bulut, 2018; Wang et al., 2024; Zhu et al., 2022) and may be influenced by the catalog completeness (Mignan, 2014). Proposed models include fluid-driven processes, slow-slip events, cascade triggering, pre-slip nucleation, or their combination (Dodge et al., 1996; Kato et al., 2012; Lei, 2024; Martínez-Garzón & Poli, 2024; Zhu et al., 2022). These models can be broadly categorized into two end-members (Gomberg, 2018): (a) the aseismically-driven model, which includes slow-slip events, fluid-driven processes or a combination of them. These aseismic processes may represent a preparation process for large earthquakes (Bouchon et al., 2011); and (b) the cascade model, where foreshocks trigger other foreshocks and the mainshock, with no intrinsic distinction in triggering mechanisms between foreshocks, mainshocks and aftershocks (Ellsworth & Bulut, 2018; Felzer et al., 2004). Distinguishing these models requires understanding the relative contributions of aseismic and seismic processes during the precursory phase. However, direct observations of aseismic slip are available for only a few cases (Gomberg, 2018; Peng & Lei, 2024). An alternative approach is to use the Epidemic-Type Aftershock Sequence (ETAS) model (Ogata, 1988), which effectively characterizes the cascade-triggering behavior and is widely applied to distinguish between aseismic-type and cascade-type foreshocks (Manganiello et al., 2023; Moutote et al., 2021). However, ETAS-based studies are inconclusive, with some favoring aseismic-type foreshocks (Petrillo & Lippiello, 2021; Seif et al., 2019) and others supporting cascade-type foreshocks (Helmstetter et al., 2003; Helmstetter & Sornette, 2003).

Here, we systematically investigate the impact of seismic monitoring capability on foreshock identification in California. Specifically, we quantify how the magnitude of completeness M_c of the catalog influences the foreshock identification results of four popular methods: the Space-Time Window (STW) method, Nearest-Neighbor Clustering (NNC) method, the Empirical Statistical (ES) method and the ETAS model. Our findings reveal that, while the STW method exhibits a strong dependence of P_f on M_c, the other approaches are largely unaffected. Our results from the ETAS model imply that high M_c may hinder the distinction between aseismic-type and cascade-type foreshocks.

2. Data

We use the relocated Southern California catalog from 1981 to 2023 and the Northern California catalog from 1984 to 2023 (Hauksson et al., 2012; Waldhauser & Schaff, 2008). To identify independent mainshocks, we apply the NNC method to events with $M \geq 1.5$ (Baiesi & Paczuski, 2004; Zaliapin et al., 2008). This method calculates a space-time-magnitude distance (η) between each event j and a previous event i:

$$\eta_{ij} = \begin{cases} t_{ij}(r_{ij})^{d_f} 10^{-bm_i} & t_{ij} < 0 \\ \infty & t_{ij} > 0 \end{cases} \quad (1)$$

where t_{ij} is the time interval between both events, r_{ij} the spatial distance, d_f the earthquake fractal dimension, b the slope of the frequency-magnitude distribution and m_i the magnitude of event i. In this study, we set $d_f = 1.6$ and $b = 1$ (Cheng & Chen, 2018; Zaliapin & Ben-Zion, 2013a, 2013b). Each event is linked to its nearest parent with the smallest η. Earthquake clusters are identified based on a threshold distance η_0 (Figure S1 in Supporting Information S1), which is determined by a Gaussian Mixture Model (Dempster et al., 1977). The largest earthquake in each cluster is designated as an independent mainshock. We focus on clusters with mainshock magnitudes $M \geq 5$.

We assess the local completeness magnitude M_c^{real} of the catalog within a 50 km radius of each mainshock epicenter over a 10-year window (5 years before and after) using the maximum curvature and Goodness-of-Fit Test (GFT) methods (Wiemer & Wyss, 2000; Woessner & Wiemer, 2005). The higher M_c^{real} value among the two

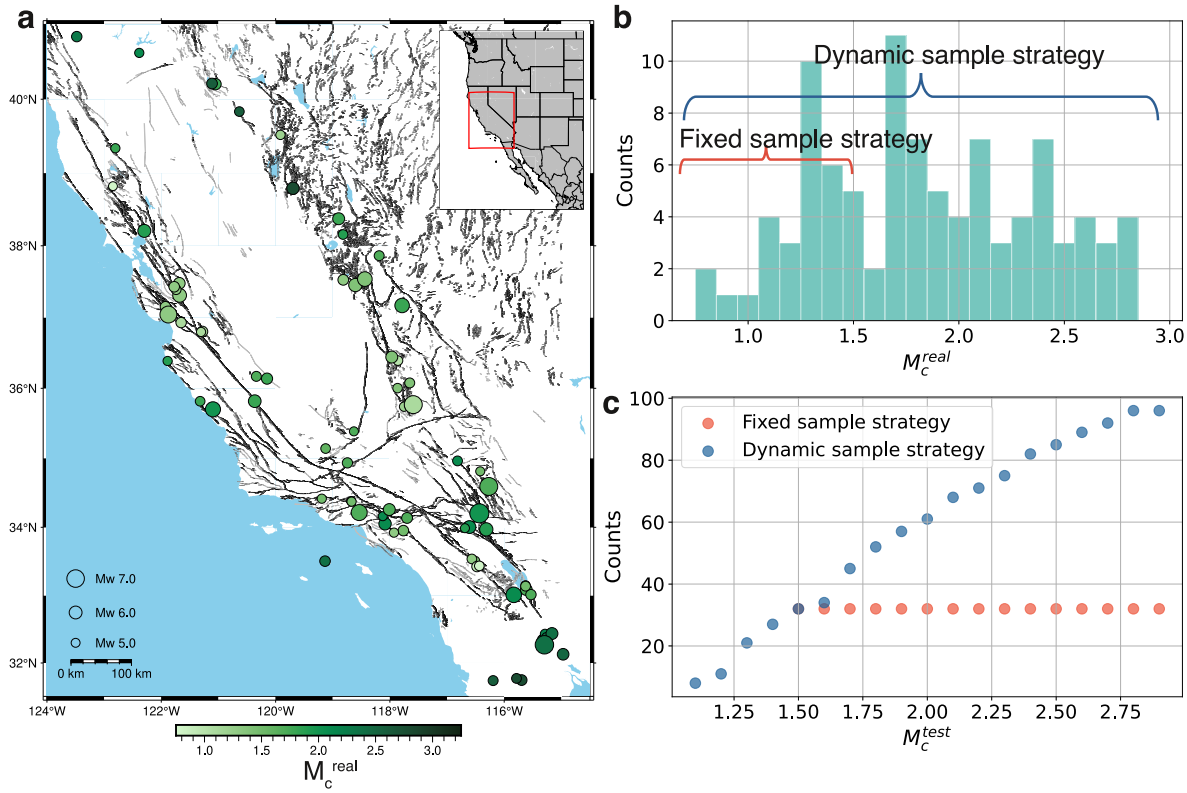

Figure 1. Map of $M > 5$ mainshocks in California from 1981 to 2023. (a) Spatial distribution of $M > 5$ mainshocks, color-coded by the magnitude of completeness (M_c^{real}) around the mainshocks. (b) Histogram of M_c^{real}. (c) Comparison of two strategies for selecting the minimum magnitude threshold (M_c^{test}). Fixed sample strategy uses a fixed sample of 30 events with $M_c^{\text{real}} \leq 1.5$, allowing M_c^{test} varying from 1.5 to 3 (red dots). Dynamic sample strategy selects events with $M_c^{\text{real}} \leq M_c^{\text{test}}$ allowing M_c^{test} to vary from 1.3 to 3.0.

methods is adopted. Sequences where M_c^{real} values differ by more than 0.5 between the two are excluded. These selections result in 97 earthquake clusters from the two relocated catalogs (Figure 1 and Table S3 in Supporting Information S1). For validation, we also analyze the 46 mainshocks with $M \geq 4$ from the QTM catalog used by Trugman and Ross (2019). See Text S1in Supporting Information S1 for more details.

3. Methods

To assess the impact of monitoring capability on foreshock identification, we simulate reduced seismic monitoring resolution by removing events below a test magnitude threshold, M_c^{test}. We adopt two strategies to select a pool of mainshock sequences to examine the proportion of foreshocks:

1. "Fixed-sample-size strategy": We keep using 32 sequences whose actual completeness magnitude satisfies the condition $M_c^{\text{real}} \leq 1.5$. Then, for each value of M_c^{test} ranging from 1.5 to 3.0, we remove small earthquakes that satisfy $M < M_c^{\text{test}}$. In this strategy, the number of sequences is 32 for values of M_c^{test} (Figure 1c).
2. "Dynamic-sample-size strategy": For each value of M_c^{test} ranging from 1.3 to 3.0, we select all sequences that satisfy $M_c^{\text{real}} \leq M_c^{\text{test}}$, then remove earthquakes with $M < M_c^{\text{test}}$. This results in an increasing number of sequences as a function of M_c^{test}, ranging from 20 to 97 sequences (Figure 1c).

The STW method identifies foreshocks as events with $M \geq M_c^{\text{test}}$ occurring within 20 days and 10 km of a mainshock (Trugman & Ross, 2019). The NNC method applies the previously described NNC approach to a smaller space-time region, targeting earthquakes with $M \geq M_c^{\text{test}}$ within a 50 km radius of the mainshock and spanning a 10-year window (5 years before and after the mainshock). Events preceding the mainshock in the same clusters are identified as foreshocks (Zaliapin & Ben-Zion, 2013b). For both methods, a mainshock is considered to have foreshocks if at least one qualifying event is detected.

The ES method evaluates foreshock activity by comparing seismicity within a short spatiotemporal window (20 days before and 10 km around the mainshock) to the long-term background activity (van den Ende & Ampuero, 2020). Background activity is estimated from 5,000 randomly selected 20-day intervals between 380 and 40 days before the mainshock. Foreshock activity is quantified by counting the number of events in the 20-day window prior to the mainshocks (N_{obs}). The probability of observing at least N_{obs} events in a random 20-day period (p_{ES}) is computed as:

$$p_{ES}(N \geq N_{obs}) = 1 - \mathrm{i}/\{\mathrm{N}\} \tag{2}$$

where i is the rank of N_{obs} within the sorted list of background earthquake counts from random 20-day windows, arranged in ascending order, and $\{N\}$ the total number of iterations (here $\{N\} = 5{,}000$). A value $p_{ES} < 0.01$ indicates statistically significant foreshock activity.

The ETAS model simulates cascade-triggering behavior through earthquake interactions. Therefore, how well an earthquake sequence is fitted by this model provides a hint for the sequence being cascade-type rather than aseismic-type (Manganiello et al., 2023; Moutote et al., 2021; Ogata, 2017; Ogata & Katsura, 2014). The seismicity rate at any given time is represented as the sum of a background rate and the rate of aftershocks triggered by past events:

$$\lambda(t) = \mu + \sum_{i|t_i<t} K e^{\alpha(M_i - M_c)}(t - t_i + c)^{-p} \tag{3}$$

where μ is the background rate, K scales aftershock productivity, the coefficient α characterizes the magnitude dependence of aftershock productivity, and the exponent p governs the temporal decay of aftershock rates. All parameters are constant over time to focus on earthquake interactions without transient aseismic forcing. We estimate the ETAS parameters using maximum likelihood estimation, and assess their uncertainties with Hessian Matrix method (Guo & Ogata, 1997; Moutote et al., 2021; Ogata, 2017). For each mainshock sequence, we select earthquakes within a 50-km radius and a 10-year window (5 years before and after the mainshock) to ensure sufficient aftershock converage and stable inverison. The ETAS parameters are estimated independently for each M_c^{test} (Figure S3 and Table S1 in Supporting Information S1).

Following Moutote et al. (2021), we compare the observed number of events (N_{obs}) with the expected number ($\overline{N}$):

$$\overline{N}(t,T) = \int_{t-T}^{t} \lambda(u)\, du \tag{4}$$

where t is the mainshock occurrence time and T the 20-day window length. The probability p_{ETAS} to have N_{obs} or more events in the ETAS model is:

$$p_{ETAS} = P(N \geq N_{obs}) = 1 - \sum_{n=0}^{N_{obs}-1} \frac{\overline{N}^n e^{-\overline{N}}}{n!} \tag{5}$$

A value $p_{ETAS} < 0.01$ indicates the presence of an aseismic forcing driving aseismic-type foreshocks.

4. Results

We found that the proportion of mainshocks with foreshocks P_f varies with the test completeness magnitude (M_c^{test}) to different degrees, depending on the foreshock identification methods (Figure 2). For the fixed-sample-size strategy (Figure 2a), the STW method shows a marked decrease in P_f as M_c^{test} increases (declining from 80% to 90% at $M_c^{test} = 1.5$ to approximately 40% at $M_c^{\mathrm{test}} = 3.0$). In contrast, the NNC and ES methods produce stable P_f values across all M_c^{test} values (~40% for NNC and 20%–30% for ES). Results from the dynamic-sample-size strategy (Figure 2b) align well with the fixed-sample-size strategy: P_f from the STW method shows a significant decreasing trend with increasing M_c^{test}, while P_f from NNC and ES methods remains generally constant or decreases slightly.

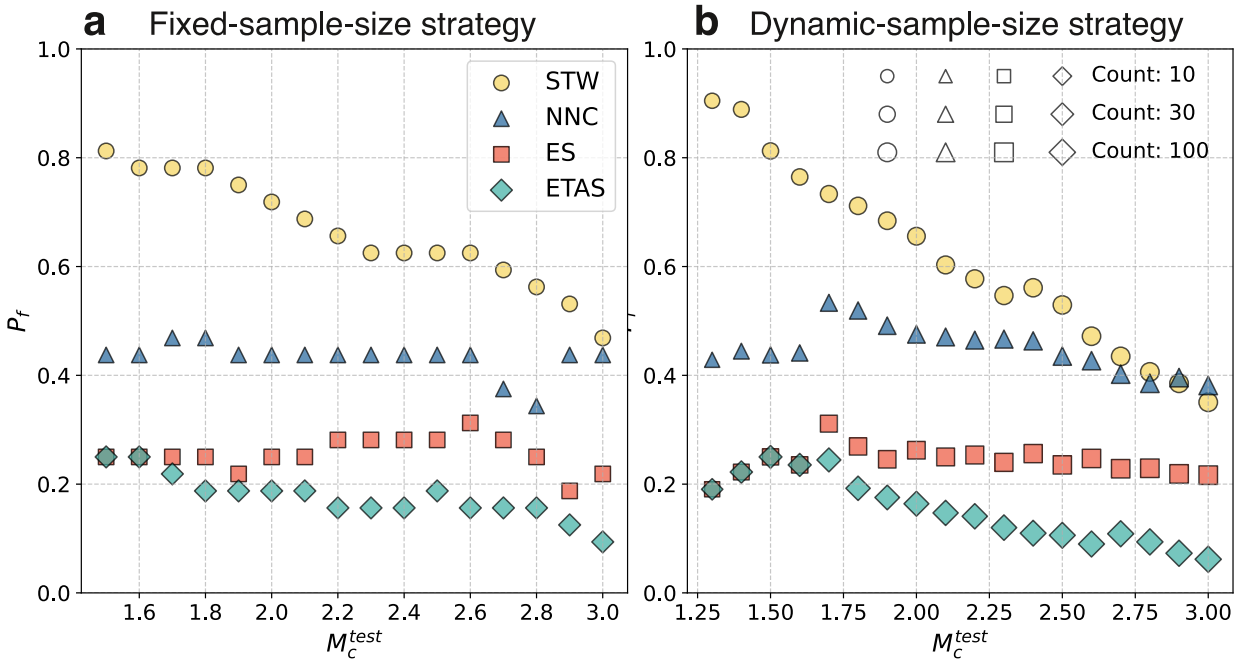

Figure 2. Dependencies of foreshock proportion (P_f) and M_c^{test} from the relocated catalogs (Hauksson et al., 2012; Waldhauser & Schaff, 2008), using (a) a fixed sample size and (b) dynamic sample sizes. Foreshock proportions are determined by different methods, including fixed window (Space-Time Window, yellow circles), Nearest neighbor clustering (NNC, blue triangles), Empirical Statistical (ES) method (ES, red squares), and epidemic-type aftershock sequence (ETAS) analysis (ETAS, green diamonds).

In the ETAS method, P_f represents the proportion of mainshocks that have aseismic-type foreshocks (Figures 3a and 3c). For cases without significant foreshock anomalies (Figure 3b) or those with cascade-type foreshocks (Figure 3d), the ETAS-based analysis does not show statistical significance ($p_{ETAS} > 0.01$). The foreshocks identified by the ETAS and ES methods are not always consistent. For example, the 17 July 2001, M5.2 Coso Junction event is classified by the ETAS method as having an aseismic-type foreshock sequence but does not pass the statistical significance test in the ES method (Figure 3c). P_f from the ETAS method in relocated catalogs shows slight decrease trend with M_c^{test} (Figure 2), aligning with previous studies indicating that lower minimum magnitudes tend to detect more aseismic-type foreshocks (Mignan, 2014).

Similar patterns are observed in the QTM catalog (Figure S4 in Supporting Information S1): the STW method shows a clear dependence of P_f on M_c^{test}, while the P_f from NNC and ES methods show weak dependencies. Moreover, the P_f obtained by the ES and ETAS methods are slightly lower in the QTM catalog than in the relocated catalog. These result contrast with the high P_f (~70%) reported by Trugman and Ross (2019), but align with van den Ende & Ampuero (2020) and Moutote et al. (2021), who found no significant improvement in P_f using the QTM catalog. The lower P_f from the ETAS in the QTM catalog may be caused by missing small earthquakes that differ from the templates (Text S1 and Figure S2 in Supporting Information S1). The difference in the ES method may arise from the larger magnitude of foreshocks, hence of foreshocks, in the relocated catalog compared to the QTM catalog, making them easier to distinguish from background events (Text S1 and Figure S5 in Supporting Information S1).

5. Discussion

5.1. Discrepancies Between the STW, NNC and ES Methods

For the events with significant foreshock activity, such as the 21 July 1986, M6.4 Chalfant Valley earthquake (Figure 3a), all three methods identify foreshocks. However, the STW method may misclassify background events as foreshocks, particularly at low M_c^{test}. This leads to an increase in P_f at low M_c^{test} (Figure 2). For example, the STW method classifies the 14 December 2016, M5 Geysers event as having foreshocks (Figure 3b), in

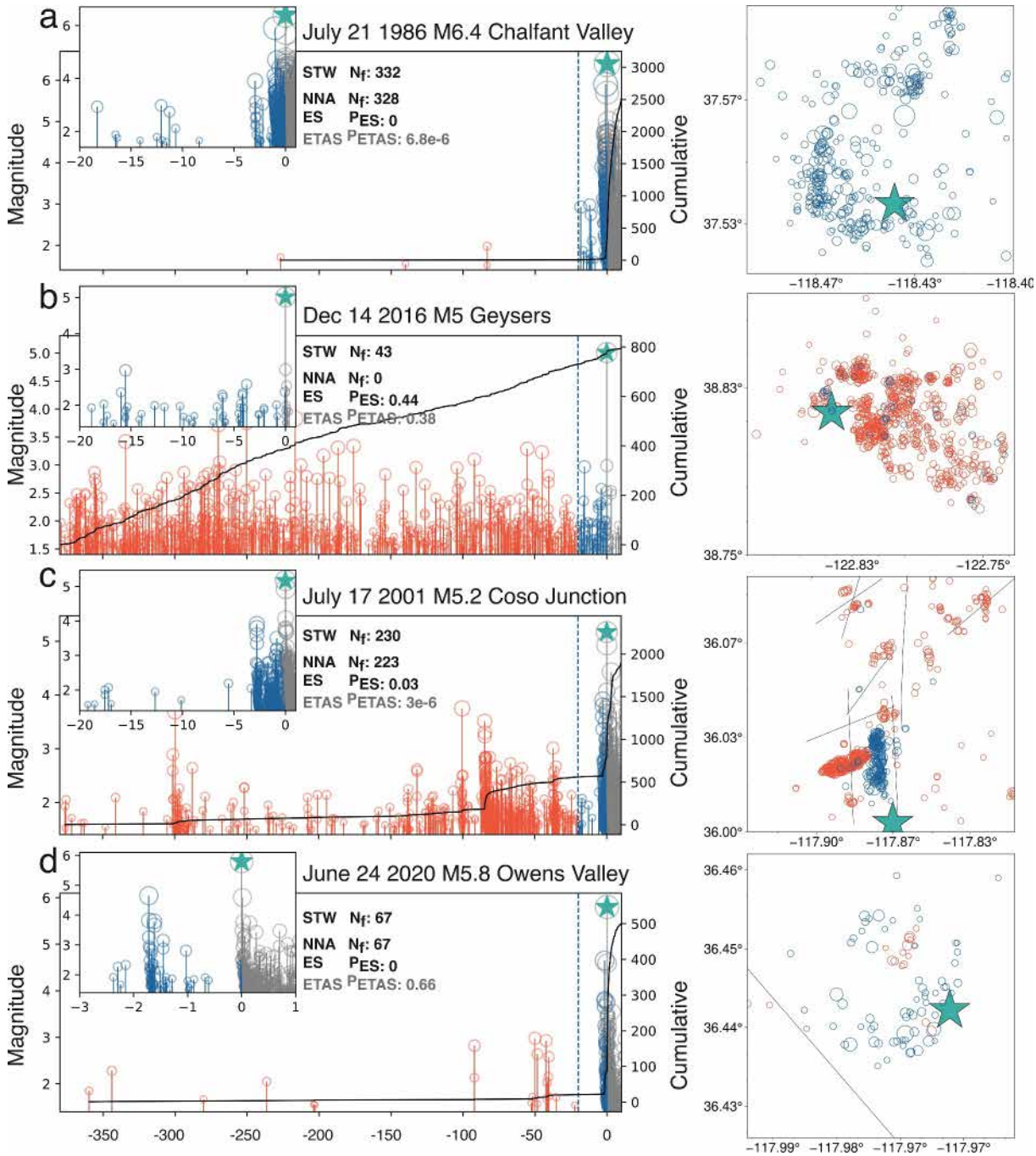

Figure 3. Spatial and temporal distribution of selected mainshocks. Left panels: Temporal distributions of earthquakes. Right panel: Spatial distribution of earthquakes. Red lines and dots represent events occurring 380 to 20 days before the mainshock, while blue lines and dots represent earthquakes occurring 20 to 0 days prior to the mainshock. Insets are a zoomed-in view of earthquakes occurring within the final 20 days. Green stars denote the mainshocks.

contrast to the other two methods which account for background seismicity. Therefore, the STW method may be unsuitable for foreshock identification in catalogs with low M_c.

The P_f value derived from the NNC method is slightly higher than that from the ES method due to different definitions of foreshocks. NNC identifies clusters based on the space-time-magnitude distance and considers foreshocks as pre-mainshock events within the same cluster, making it less sensitive to background activity. In contrast, ES detects foreshocks as significant increases in seismicity compared to the background activity. As a

result, events with high background seismicity, such as the 17 July 2021, M5.2 Coso event (Figure 3c), are identified as having foreshocks by the NNC method, but not by the ES method. This discrepancy can be reduced by loosening the threshold of p_{ES}: with a threshold of 0.1, the ES method produces results more consistent with the NNC method (Figure S6 in Supporting Information S1).

To further evaluate their performance, we use the ETAS model to generate synthetic catalogs with known "ground truth", that is, in which mainshocks ($M \geq 5$) that have foreshocks are explicitly identified (Text S2 in Supporting Information S1). In these catalogs, approximately 50% of mainshocks have foreshocks. While these synthetic catalogs are simpler than real ones and do not capture all complexities such as transient aseismic processes, they provide a valuable benchmark for assessing the methods performance. The NNC method achieves 82% accuracy, while the ES method performs worse (65% accuracy), miss more sequences with small-magnitude foreshocks (Figure S7 in Supporting Information S1). These results suggest that the NNC method can exploit small earthquakes better than the ES method.

Both methods have their own strengths: For studying small-magnitude mainshocks, which has become increasingly popular due to improvement in seismic networks and detection methods (Beroza et al., 2021; Li, 2021a, 2021b), the NNC method is more effective as it may detect foreshock activity within a globally high level of background seismicity. Conversely, for short-term earthquake forecasting, where strict metrics are necessary to minimize false predictions (Zaccagnino et al., 2024), the ES method is more suitable. Moreover, as the NNC method relies on entire clusters to define foreshocks, it is inherently restricted to retrospective analyses and is unsuitable for real-time forecasting scenarios. To address these limitations, for the NNC method, integrating clustering-based approaches with techniques like supervised learning (Cui et al., 2024) might improve its predictive capabilities.

5.2. Magnitude Difference Between the Largest Foreshocks and Mainshocks

The estimated proportions of mainshocks with foreshocks, P_f, derived from both the NNC and ES methods remain largely constant with improved detection capability, suggesting that the magnitude difference between mainshocks and their largest foreshock (ΔM_{mf}) is typically small in the analyzed data; otherwise, raising M_c^{test} would cause a noticeable decrease in P_f.

Previous studies of ΔM_{mf} have reported contradictory results: some suggest the ΔM_{mf} distribution is relatively uniform (Michael & Jones, 1998; Reasenberg, 1999), while others proposed that small ΔM_{mf} values are more common (Agnew & Jones, 1991; Lindh & Lim, 1995). However, these analyzes focus on a narrow range between M_c and mainshock magnitude (mostly around 2). We analyze 14 sequences with foreshocks identified by the NNC method (Figure 4a). The results show that ΔM_{mf} is typically smaller than 2 (Figure 4b). Therefore, most mainshocks retain detectable foreshocks as M_c^{test} increases, which explains the stable P_f from NNC and ES methods. To assess whether this narrow magnitude is influenced by biases from the differences between mainshock magnitude and M_c, we compare the magnitude differences for events with and without foreshocks (Figure S8 in Supporting Information S1). The nearly identical distributions suggest that M_c has a minimal influence on the observed trend.

In the ETAS framework, the dependence of P_f on M_c is governed by the difference between the ETAS model parameter α and the Gutenberg-Richter parameter β. α characterizes the magnitude dependence of aftershock productivity, and $\beta = b \times \ln(10)$, characterizes the exponential decay of the Gutenberg-Richter frequency distribution (Gutenberg & Richter, 1944). The total number of earthquakes triggered by events of magnitude m scales as $10^{(\alpha-\beta)m}$ (Helmstetter, 2003). When $\alpha < \beta$, small earthquakes dominate triggering, and lowering M_c is expected to increase the fraction of large events with detectable foreshocks. Figure S3b in Supporting Information S1 shows that most sequences exhibit $\alpha - \beta < 0$, consistent with previous analyses in California (Helmstetter, 2003; Nandan et al., 2017). However, this expectation is at odds with our observation of a constant P_f when varying M_c^{test} for the NNC and ES methods.

To investigate this discrepancy, we generate synthetic catalogs with $\alpha = 1.7$ and $\beta = 2.3$ ($b = 1$) based on previous studies (Mizrahi et al., 2021) and our observed α - β values (Figure S3b; see Text S2 in Supporting Information S1 for more details). As expected for $\alpha < \beta$, the synthetic sequences show large magnitude differences between the mainshock and its largest foreshock (Figure 4b and Figure S9 in Supporting Information S1), different from the

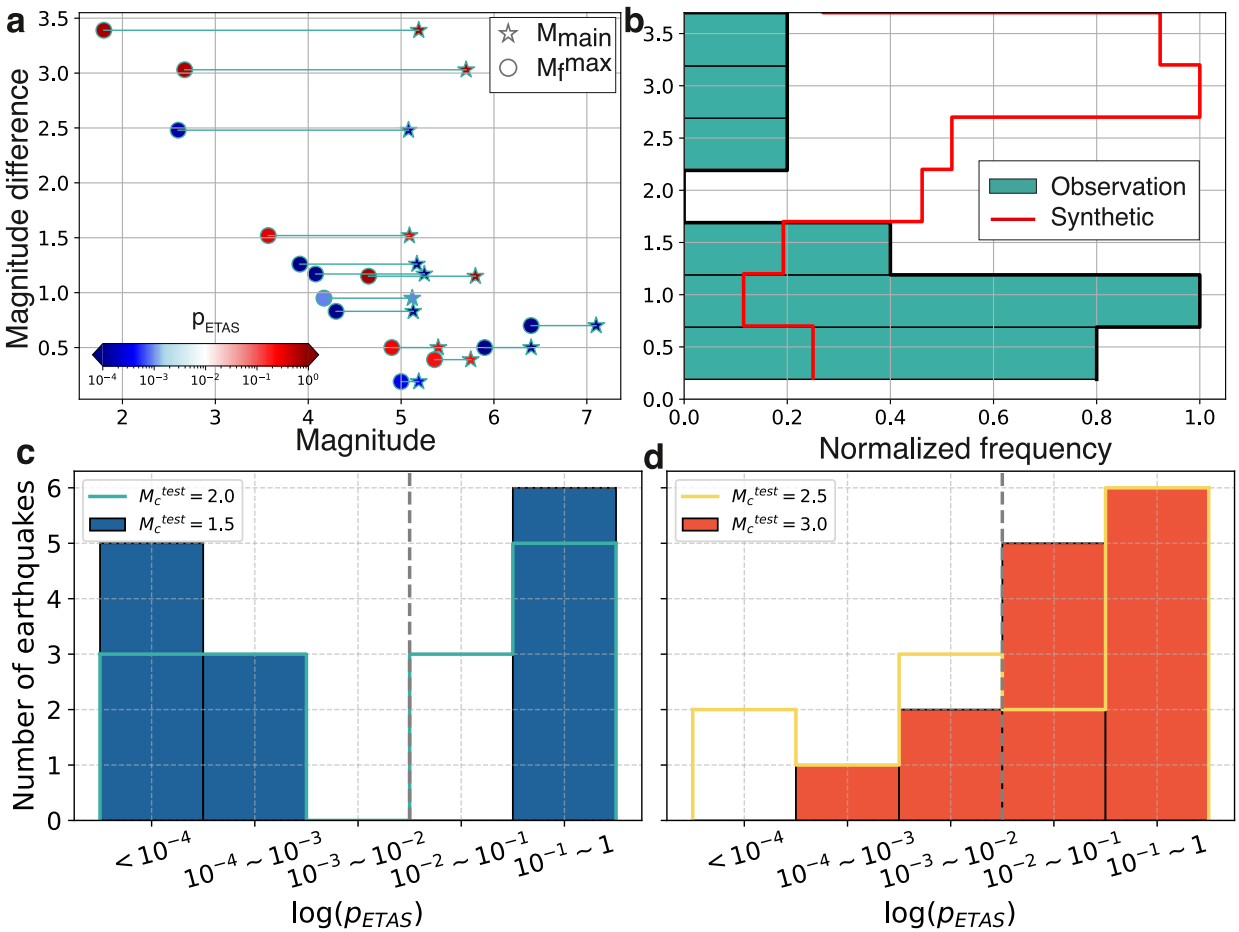

Figure 4. Magnitude differences between mainshocks and their largest foreshocks. (a) Scatter plot of magnitudes of mainshocks (stars) and their largest foreshocks (circles) detected by the Nearest-Neighbor Clustering at $M_c^{\text{test}} = 1.5$. Colors indicate p_{ETAS} values derived from ETAS: white and blue colors ($p_{ETAS} \leq 0.01$) correspond here to aseismic-type foreshocks. (b) Distribution of magnitude differences, normalized to a maximum of 1, for observed events in the California earthquake catalog (green) and ETAS-simulated catalogs (red). (c) Histogram of p_{ETAS} at $M_c^{\text{test}} = 1.5$ (blue) and 2 (green). (d) Histogram of p_{ETAS} at $M_c^{\text{test}} = 2.5$ (yellow) and 3 (red).

observed sequences in California (Figure 4). Notably, many sequences with small magnitude differences are associated with $p_{\text{ETAS}} < 0.01$, suggesting foreshocks related to aseismic processes (Figure 4a). Thus, the discrepancy indicates that the constant P_f value and small magnitude difference are likely due to the contribution of aseismic processes to some foreshock sequences, consistent with previous findings (Chen & Shearer, 2013; Petrillo & Lippiello, 2021). Chen and Shearer (2013) reported widespread aseismic-type foreshocks in California. Petrillo and Lippiello (2021) showed that ETAS models underpredict the number of events preceding the mainshocks ($M \geq 5$) observed in California, implying the presence of additional triggering mechanisms.

5.3. ETAS Model Evaluation With Varying M_c^{test}

At $M_c^{\text{test}} = 1.5$, among the 14 sequences with foreshocks identified by the NNC method, more than half (8) have $p_{\text{ETAS}} < 0.01$, which are classified as aseismic-type foreshocks; the remaining 6 are classified as cascade-type foreshocks. As M_c^{test} increases, the p_{ETAS} value of the original 8 aseismic-type foreshock sequences tend to rise, often exceeding 0.01, whereas the original 6 cascade-type foreshocks show a slight decrease of p_{ETAS} (Figures 4c and 4d and S10). Consequently, at higher M_c^{test}, fewer sequences are classified as aseismic-type. Thus, the ETAS model's ability to distinguish between the two foreshock types diminishes as M_c^{test} increases, which may be due to: (a) a smaller number of events available for ETAS parameter inversion, which increases uncertainty (Table S1 in Supporting Information S1); and (b) fewer small events, which limits the branching information needed for distinguishing aseismic-type foreshocks. The diminishing distinction at high M_c^{test} possibly explains the inconsistencies in the interpretation of the foreshock types in many previous studies. Studies reporting that

pre-slip and cascade processes are indistinguishable from ETAS modeling typically use catalogs with high Mc (Felzer et al., 2004; Helmstetter et al., 2003; Helmstetter & Sornette, 2003), while those attributing foreshocks to aseismic slip often use catalogs with low M_c (Chen & Shearer, 2016; Petrillo & Lippiello, 2021; Seif et al., 2019).

Our results suggest that catalogs that are complete down to smaller magnitudes help distinguish better aseismic-type foreshocks from cascade-type foreshocks, but they do not substantially improve the capacity to identify whether a mainshock has foreshocks. More complete catalogs are also useful for other purposes. They can enable a more accurate tracking of changes of b-values, which can enhance short-term earthquake forecasting in traffic-light systems (Gulia & Wiemer, 2019). Additionally, small earthquakes can better capture the spatiotemporal evolution and migration speed of earthquake sequences, offering key insights into the underlying aseismic processes (Danré et al., 2022, 2024; Ellsworth & Bulut, 2018; Peng & Lei, 2024). Moreover, incorporating estimates of additional source properties into the analysis, such as stress drop, may further enhance the detection and interpretation of foreshock activity (Chen & Shearer, 2013; Socquet et al., 2017).

6. Conclusions

We systematically evaluated the impact of seismic monitoring capability on the proportion of mainshocks identified as having foreshocks (P_f) in California. By examining four foreshock identification methods, we find that the dependence of P_f on the catalog completeness magnitude (M_c) is weak for NNC and empirical statistic methods (ES). This consistency likely arises from the typically small magnitude differences between mainshocks and their largest foreshock in moderate earthquake in California. In contrast, the fixed-window method shows a strong anti-correlation between P_f and M_c, primarily due to its overlook of background fluctuations. Discrepancies between the NNC and ES methods stem from their different definitions of foreshocks, with ES methods excluding sequences with a rate similar to the background seismicity level. Epidemic-type aftershock sequence model analysis further shows that improved detection of small earthquakes enhances the model's ability to distinguish aseismic-type foreshocks from cascade-type foreshocks. Our results suggest that improving seismic monitoring capability may not significantly improve estimations of the pervasiveness of foreshocks, but is crucial for accurately identifying foreshock types.

The ETAS analysis further reveals that $\alpha - \beta < 0$ for most mainshock sequences in California, suggesting that small earthquakes dominate triggering. This contrasts with the observed weak dependence of P_f on M_c and the small magnitude differences between mainshocks and their largest foreshocks. Moreover, more than half of the foreshock sequences cannot be fully explained by the ETAS model, implying that aseismic processes likely play a significant role for those sequences in California.

Conflict of Interest

The authors declare no conflicts of interest relevant to this study.

Data Availability Statement

The Southern California catalog of Hauksson et al. (2012) was obtained from https://scedc.caltech.edu/data/alt-2011-dd-hauksson-yang-shearer.html, version "1981–2023" (last accessed October 2024). The Northern California catalog of Waldhauser & Schaff, 2008 was obtained from https://www.ncedc.org/ncedc/catalog-search.html, from 1984 to 2023 (last accessed October 2024). The QTM seismicity catalog accessible via the Southern California Earthquake Data Center (https://scedc.caltech.edu/data/qtm-catalog.html; last accessed October 2024).

Acknowledgments
We thank the Editor Germán Prieto, the anonymous Associate Editor and two anonymous reviewers for their constructive comments. This work was supported by the National Natural Science Foundation of China (no. 42274063 and no. 4248830017). Xin Cui was supported by Youth Student Basic Research Project (PhD Student), National Natural Science Foundation of China (GG2080000765) and by the Outstanding PhD International Exchange Program of the University of Science and Technology of China. J.P.A. was supported by the French government through the UCAJEDI Investments in the Future project (ANR-15-IDEX-01) managed by the National Research Agency (ANR).

References

Abercrombie, R. E., & Mori, J. (1996). Occurrence patterns of foreshocks to large earthquakes in the Western United States. *Nature*, *381*(6580), 303–307. https://doi.org/10.1038/381303a0

Agnew, D. C., & Jones, L. M. (1991). Prediction probabilities from foreshocks. *Journal of Geophysical Research*, *96*(B7), 11959–11971. https://doi.org/10.1029/91JB00191

Ampuero, J.-P., & Rubin, A. M. (2008). Earthquake nucleation on rate and state faults–Aging and slip laws. *Journal of Geophysical Research*, *113*(B1), B01302. https://doi.org/10.1029/2007JB005082

Baiesi, M., & Paczuski, M. (2004). Scale-free networks of earthquakes and aftershocks. *Physical Review*, *6*(9), 066106.

Beroza, G. C., Segou, M., & Mostafa Mousavi, S. (2021). Machine learning and earthquake forecasting—Next steps. *Nature Communications*, *12*(1), 4761. https://doi.org/10.1038/s41467-021-24952-6

Bolton, D. C., Shokouhi, P., Rouet-Leduc, B., Hulbert, C., Rivière, J., Marone, C., & Johnson, P. A. (2019). Characterizing acoustic signals and searching for precursors during the laboratory seismic cycle using unsupervised machine learning. *Seismological Research Letters*, *90*(3), 1088–1098. https://doi.org/10.1785/0220180367

Bouchon, M., Karabulut, H., Aktar, M., Özalaybey, S., Schmittbuhl, J., & Bouin, M.-P. (2011). Extended nucleation of the 1999 M_w 7.6 izmit earthquake. *Science*, *331*(6019), 877–880. https://doi.org/10.1126/science.1197341

Chen, X., & Shearer, P. M. (2013). California foreshock sequences suggest aseismic triggering process. *Geophysical Research Letters*, *40*(11), 2602–2607. https://doi.org/10.1002/grl.50444

Chen, X., & Shearer, P. M. (2016). Analysis of foreshock sequences in California and implications for earthquake triggering. *Pure and Applied Geophysics*, *173*(1), 133–152. https://doi.org/10.1007/s00024-015-1103-0

Cheng, Y., & Chen, X. (2018). Characteristics of seismicity inside and outside the salton sea geothermal field. *Bulletin of the Seismological Society of America*, *108*(4), 1877–1888. https://doi.org/10.1785/0120170311

Cui, X., Hu, Y., Ma, S., Li, Z., Liu, G., & Huang, H. (2024). Bridging supervised and unsupervised learning to build volcano seismicity classifiers at Kilauea volcano, Hawaii. *Seismological Research Letters*, *95*(3), 1849–1857. https://doi.org/10.1785/0220230251

Danré, P., De Barros, L., Cappa, F., & Ampuero, J. P. (2022). Prevalence of aseismic slip linking fluid injection to natural and anthropogenic seismic swarms. *Journal of Geophysical Research: Solid Earth*, *127*(12), e2022JB025571. https://doi.org/10.1029/2022jb025571

Danré, P., De Barros, L., Cappa, F., & Passarelli, L. (2024). Parallel dynamics of slow slips and fluid-induced seismic swarms. *Nature Communications*, *15*(1), 8943. https://doi.org/10.1038/s41467-024-53285-3

Dempster, A. P., Laird, N. M., & Rubin, D. B. (1977). Maximum likelihood from incomplete data via the EM algorithm. *Journal of the Royal Statistical Society: Series B*, *39*(1), 1–22. https://doi.org/10.1111/j.2517-6161.1977.tb01600.x

Dieterich, J. (1994). A constitutive law for rate of earthquake production and its application to earthquake clustering. *Journal of Geophysical Research*, *99*(B2), 2601–2618. https://doi.org/10.1029/93JB02581

Dodge, D. A., Beroza, G. C., & Ellsworth, W. L. (1995). Foreshock sequence of the 1992 Landers, California, earthquake and its implications for earthquake nucleation. *Journal of Geophysical Research*, *100*(B6), 9865–9880. https://doi.org/10.1029/95JB00871

Dodge, D. A., Beroza, G. C., & Ellsworth, W. L. (1996). Detailed observations of California foreshock sequences: Implications for the earthquake initiation process. *Journal of Geophysical Research*, *101*(B10), 22371–22392. https://doi.org/10.1029/96JB02269

Ellsworth, W. L., & Bulut, F. (2018). Nucleation of the 1999 Izmit earthquake by a triggered cascade of foreshocks. *Nature Geoscience*, *11*(7), 531–535. https://doi.org/10.1038/s41561-018-0145-1

Felzer, K. R., Abercrombie, R. E., & Ekström, G. (2004). A common origin for aftershocks, foreshocks, and multiplets. *Bulletin of the Seismological Society of America*, *94*(1), 88–98. https://doi.org/10.1785/0120030069

Goebel, T. H. W., Schuster, V., Kwiatek, G., Pandey, K., & Dresen, G. (2024). A laboratory perspective on accelerating preparatory processes before earthquakes and implications for foreshock detectability. *Nature Communications*, *15*(1), 5588. https://doi.org/10.1038/s41467-024-49959-7

Gomberg, J. (2018). Unsettled earthquake nucleation. *Nature Geoscience*, *11*(7), 463–464. https://doi.org/10.1038/s41561-018-0149-x

Gulia, L., & Wiemer, S. (2019). Real-time discrimination of earthquake foreshocks and aftershocks. *Nature*, *574*(7777), 193–199. https://doi.org/10.1038/s41586-019-1606-4

Guo, Z., & Ogata, Y. (1997). Statistical relations between the parameters of aftershocks in time, space, and magnitude. *Journal of Geophysical Research*, *102*(B2), 2857–2873. https://doi.org/10.1029/96jb02946

Gutenberg, B., & Richter, C. F. (1944). Frequency of earthquakes in California. *Bulletin of the Seismological Society of America*, *34*(4), 185–188. https://doi.org/10.1785/bssa0340040185

Hauksson, E., Yang, W., & Shearer, P. M. (2012). Waveform relocated earthquake catalog for Southern California (1981 to June 2011) [Dataset]. *Bulletin of the Seismological Society of America*, *102*(5), 2239–2244. https://doi.org/10.1785/0120120010

He, C., Zhang, L., Liu, P., & Chen, Q.-F. (2023). Characterizing the final stage of simulated earthquake nucleation governed by rate-and-state fault friction. *Journal of Geophysical Research: Solid Earth*, *128*(5), e2023JB026422. https://doi.org/10.1029/2023JB026422

Helmstetter, A. (2003). Is earthquake triggering driven by small earthquakes? *Physical Review Letters*, *91*(5), 058501.

Helmstetter, A., & Sornette, D. (2003). Foreshocks explained by cascades of triggered seismicity. *Journal of Geophysical Research*, *108*(B10), 2003JB002409. https://doi.org/10.1029/2003JB002409

Helmstetter, A., Sornette, D., & Grasso, J.-R. (2003). Mainshocks are aftershocks of conditional foreshocks: How do foreshock statistical properties emerge from aftershock laws. *Journal of Geophysical Research*, *108*(B1), 2046. https://doi.org/10.1029/2002JB001991

Kato, A., Obara, K., Igarashi, T., Tsuruoka, H., Nakagawa, S., & Hirata, N. (2012). Propagation of slow slip leading up to the 2011 M_w 9.0 Tohoku-Oki earthquake. *Science*, *335*(6069), 705–708. https://doi.org/10.1126/science.1215141

Lei, X. (2024). Fluid-driven fault nucleation, rupture processes, and permeability evolution in oshima granite—Preliminary results and acoustic emission datasets. *Geohazard Mechanics*, *2*(3), 164–180. https://doi.org/10.1016/j.ghm.2024.04.003

Li, Z. (2021a). Recent advances in earthquake monitoring I: Ongoing revolution of seismic instrumentation. *Earthquake Science*, *34*(2), 177–188. https://doi.org/10.29382/eqs-2021-0011

Li, Z. (2021b). Recent advances in earthquake monitoring II: Emergence of next-generation intelligent systems. *Earthquake Science*, *34*(6), 531–540. https://doi.org/10.29382/eqs-2021-0054

Lindh, A. G., & Lim, M. R. (1995). *A clarification, correction, and updating of Parkfield, California, earthquake prediction scenarios and response plans (USGS Open-File Report 87-192) (No. 95–695)*. Open-File Report. Deptartmrnt of the Interior. U.S. Geological Survey. https://doi.org/10.3133/ofr95695

Manganiello, E., Herrmann, M., & Marzocchi, W. (2023). New physical implications from revisiting foreshock activity in Southern California. *Geophysical Research Letters*, *50*(1), e2022GL098737. https://doi.org/10.1029/2022GL098737

Martínez-Garzón, P., & Poli, P. (2024). Cascade and pre-slip models oversimplify the complexity of earthquake preparation in nature. *Communications Earth and Environment*, *5*(1), 120. https://doi.org/10.1038/s43247-024-01285-y

Marty, S., Schubnel, A., Bhat, H. S., Aubry, J., Fukuyama, E., Latour, S., et al. (2023). Nucleation of laboratory earthquakes: Quantitative analysis and scalings. *Journal of Geophysical Research: Solid Earth*, *128*(3), e2022JB026294. https://doi.org/10.1029/2022JB026294

Michael, A. J., & Jones, L. M. (1998). Seismicity alert probabilities at Parkfield, California, revisited. *Bulletin of the Seismological Society of America*, *88*(1), 117–130. https://doi.org/10.1785/BSSA0880010117

Mignan, A. (2014). The debate on the prognostic value of earthquake foreshocks: A meta-analysis. *Scientific Reports*, *4*(1), 4099. https://doi.org/10.1038/srep04099

Mizrahi, L., Nandan, S., & Wiemer, S. (2021). The effect of declustering on the size distribution of mainshocks. *Seismological Society of America*, *92*(4), 2333–2342. https://doi.org/10.1785/0220200231

Mogi, K. (1963). Some discussions on aftershocks, foreshocks and earthquake swarms-the 1151 fracture of a semi finite body caused by an inner stress origin and its relation to the earthquake 1152 phenomena. *Bulletin of the Earthquake Research Institute*, *41*, 615–658.
Moutote, L., Marsan, D., Lengliné, O., & Duputel, Z. (2021). Rare occurrences of non-cascading foreshock activity in Southern California. *Geophysical Research Letters*, *48*(7), e2020GL091757. https://doi.org/10.1029/2020GL091757
Nandan, S., Ouillon, G., Wiemer, S., & Sornette, D. (2017). Objective estimation of spatially variable parameters of epidemic type aftershock sequence model: Application to California. *Journal of Geophysical Research: Solid Earth*, *122*(7), 5118–5143. https://doi.org/10.1002/2016jb013266
Ogata, Y. (1988). Statistical models for earthquake occurrences and residual analysis for point processes. *Journal of the American Statistical Association*, *83*(401), 9–27. https://doi.org/10.1080/01621459.1988.10478560
Ogata, Y. (2017). Statistics of earthquake activity: Models and methods for earthquake predictability studies. *Annual Review of Earth and Planetary Sciences*, *45*(1), 497–527. https://doi.org/10.1146/annurev-earth-063016-015918
Ogata, Y., & Katsura, K. (2014). Comparing foreshock characteristics and foreshock forecasting in observed and simulated earthquake catalogs. *Journal of Geophysical Research: Solid Earth*, *119*(11), 8457–8477. https://doi.org/10.1002/2014JB011250
Ogata, Y., Utsu, T., & Katsura, K. (1995). Statistical features of foreshocks in comparison with other earthquake clusters. *Geophysical Journal International*, *121*(1), 233–254. https://doi.org/10.1111/j.1365-246x.1995.tb03524.x
Peng, Z., & Lei, X. (2024). Physical mechanisms of earthquake nucleation and foreshocks: Cascade triggering, aseismic slip, or fluid flows? *Earthquake Research Advances*, *5*(2), 100349. https://doi.org/10.1016/j.eqrea.2024.100349
Petrillo, G., & Lippiello, E. (2021). Testing of the foreshock hypothesis within an epidemic like description of seismicity. *Geophysical Journal International*, *225*(2), 1236–1257. https://doi.org/10.1093/gji/ggaa611
Reasenberg, P. A. (1999). Foreshock occurrence before large earthquakes. *Journal of Geophysical Research*, *104*(B3), 4755–4768. https://doi.org/10.1029/1998JB900089
Ross, Z. E., Trugman, D. T., Hauksson, E., & Shearer, P. M. (2019). Searching for hidden earthquakes in Southern California [Dataset]. *Science*, *364*(6442), 767–771. https://doi.org/10.1126/science.aaw6888
Rubin, A. M., & Ampuero, J.-P. (2005). Earthquake nucleation on (aging) rate and state faults: Rate and state earthquake nucleation. *Journal of Geophysical Research*, *110*(B11), B11312. https://doi.org/10.1029/2005JB003686
Ruiz, S., Metois, M., Fuenzalida, A., Ruiz, J., Leyton, F., Grandin, R., et al. (2014). Intenseforeshocks and a slow slip event preceded the 2014 Iquique M_w 8.1 earthquake. *Science*, *345*(6201), 1165–1169. https://doi.org/10.1126/science.1256074
Seif, S., Zechar, J. D., Mignan, A., Nandan, S., & Wiemer, S. (2019). Foreshocks and their potential deviation from general seismicity. *Bulletin of the Seismological Society of America*, *109*(1), 1–18. https://doi.org/10.1785/0120170188
Socquet, A., Valdes, J. P., Jara, J., Cotton, F., Walpersdorf, A., Cotte, N., et al. (2017). An 8 month slow slip event triggers progressive nucleation of the 2014 Chile megathrust. *Geophysical Research Letters*, *44*(9), 4046–4053. https://doi.org/10.1002/2017gl073023
Trugman, D. T., & Ross, Z. E. (2019). Pervasive foreshock activity across southern California. *Geophysical Research Letters*, *46*(15), 8772–8781. https://doi.org/10.1029/2019GL083725
van den Ende, M. P. A., & Ampuero, J.-P. (2020). On the statistical significance of foreshock sequences in Southern California. *Geophysical Research Letters*, *47*(3), e2019GL086224. https://doi.org/10.1029/2019GL086224
Waldhauser, F., & Schaff, D. P. (2008). Large-scale relocation of two decades of Northern California seismicity using cross-correlation and double-difference methods [Dataset]. *Journal of Geophysical Research*, *113*(B8), B08311. https://doi.org/10.1029/2007JB005479
Wang, K., Chen, Q.-F., Sun, S., & Wang, A. (2006). Predicting the 1975 haicheng earthquake. *Bulletin of the Seismological Society of America*, *96*(3), 757–795. https://doi.org/10.1785/0120050191
Wang, K., Peng, Z., Liang, S., Luo, J., Zhang, K., & He, C. (2024). Migrating foreshocks driven by a slow slip event before the 2021 M_W 6.1 Yangbi, China earthquake. *Journal of Geophysical Research: Solid Earth*, *129*(1), e2023JB027209. https://doi.org/10.1029/2023JB027209
Wetzler, N., Lay, T., & Brodsky, E. E. (2023). Global characteristics of observable foreshocks for large earthquakes. *Seismological Research Letters*, *94*(5), 2313–2325. https://doi.org/10.1785/0220220397
Wiemer, S., & Wyss, M. (2000). Minimum magnitude of completeness in earthquake catalogs: Examples from Alaska, the Western United States, and Japan. https://doi.org/10.1785/0119990114
Woessner, J., & Wiemer, S. (2005). Assessing the quality of earthquake catalogues: Estimating the magnitude of completeness and its uncertainty. *Bulletin of the Seismological Society of America*, *95*(2), 684–698. https://doi.org/10.1785/0120040007
Zaccagnino, D., Vallianatos, F., Michas, G., Telesca, L., & Doglioni, C. (2024). Are foreshocks fore-shocks? *Journal of Geophysical Research: Solid Earth*, *129*(2), e2023JB027337. https://doi.org/10.1029/2023JB027337
Zaliapin, I., & Ben-Zion, Y. (2013a). Earthquake clusters in Southern California I: Identification and stability: Identification of earthquake clusters. *Journal of Geophysical Research: Solid Earth*, *118*(6), 2847–2864. https://doi.org/10.1002/jgrb.50179
Zaliapin, I., & Ben-Zion, Y. (2013b). Earthquake clusters in Southern California II: Classification and relation to physical properties of the crust: Classification of earthquake clusters. *Journal of Geophysical Research: Solid Earth*, *118*(6), 2865–2877. https://doi.org/10.1002/jgrb.50178
Zaliapin, I., Gabrielov, A., Keilis-Borok, V., & Wong, H. (2008). Clustering analysis of seismicity and aftershock identification. *Physical Review Letters*, *101*(1), 018501. https://doi.org/10.1103/PhysRevLett.101.018501
Zhu, G., Yang, H., Tan, Y. J., Jin, M., Li, X., & Yang, W. (2022). The cascading foreshock sequence of the Ms 6.4 Yangbi earthquake in Yunnan, China. *Earth and Planetary Science Letters*, *591*, 117594. https://doi.org/10.1016/j.epsl.2022.117594

References From the Supporting Information

Utsu, T., & Ogata, Y. (1995). The centenary of the Omori formula for a decay law of aftershock activity. *Journal of Physics of the Earth*, *43*(1), 1–33. https://doi.org/10.4294/jpe1952.43.1
Zhuang, J., Ogata, Y., & Vere-Jones, D. (2004). Analyzing earthquake clustering features by using stochastic reconstruction. *Journal of Geophysical Research: Solid Earth*, *109*(B5), B05301. https://doi.org/10.1029/2003JB002879